Look-ahead Vehicle Energy Management with Traffic Predictions ⋆

Lars Johannesson * **Magnus Nilsson** ** **Nikolce Murgovski** ***

* *Viktoria Swedish ICT, Lindholmspiren 3A, 417 56 Göteborg, Sweden, (e-mail: larsjo@chalmers.se,lars.johannesson@viktoria.se).*
** *Viktoria Swedish ICT, Lindholmspiren 3A, 417 56 Göteborg, Sweden, (e-mail: magnus.nilsson@viktoria.se).*
*** *Chalmers University of Technology, Hörsalsvägen 11, 412 96 Göteborg, Sweden, (e-mail: nikolce.murgovski@chalmers.se)*

Abstract: This paper presents a vehicle energy management system that uses information about upcoming topography and speed limits along the planned route to schedule the speed and the gear shifts of a heavy diesel truck. The proposed control scheme divides the predictive control problem into two layers that operate with different update frequencies and prediction horizons. The focus in the paper is on the top layer that plans the vehicle speed in a convex optimization problem leaving the gear decision to be optimized in the lower layer in a dynamic program. The paper describes how predictive information of the movement pattern of surrounding vehicles can be incorporated into the convex optimization of the vehicle speed by using a moving time window constraint.

Keywords: Vehicle Energy Management, Automotive control, Long haulage truck, Predictive control, Intelligent Cruise Control

1. INTRODUCTION

Recent studies show that eco-driving can reduce the energy consumption and CO2 emissions of transporting people and goods with up to 10% Barkenbus (2010). For heavy-duty trucks eco-driving primarily means proper gear selection and utilizing a narrow over and under speed interval as a kinetic energy buffer, thereby reducing the energy dissipated in the brakes. With the likely increase in the number of vehicles that drive with radar assisted cruise control the fuel saving potential of eco-driving and eco-cruising technologies is increasing.

Several vehicle manufacturers currently provide cruise controllers that save fuel by utilizing information about the upcoming topography, controlling the speed over a receding horizon. Typically, these cruise controllers reduce the speed while climbing uphill and then roll over the crescent and during the downslope. When the topographic profile is relatively simple this behavior can be implemented with heuristic control strategies but if the topographic profile is more complex it is preferable to use a predictive controller that is based on optimal control as in Van Keulen et al. (2010, 2011); Hellström et al. (2009). As will be shown in this paper, relying on optimal control techniques have an additional advantage in that it is possible to expand the controller with information about the movement pattern of surrounding traffic.

Due to their nonconvex nature, it is most straightforward to apply dynamic programming (DP) (Bellman and Dreyfus, 1962) to solve the optimal control problems. A real-time implementable DP-algorithm that decides the gear shifts and the vehicle speed for conventional trucks is presented in Hellström et al. (2009, 2010). The DP-algorithm is able to enforce a constraint on the trip time by using a time penalty and achieves close to optimal fuel consumption for all types of topographic profiles.

However, DP suffers from the curse of dimensionality (Bertsekas, 2000), which means that computation time grows exponentially with the number of states and control signals. Additional states are required in order to include predictions of slowly moving traffic in front of the truck, additional energy storages due to hybridization and predictive control of the auxiliary systems, see Pettersson and Johansson (2006); Koot et al. (2005).

To overcome the computational limitations of DP, Johannesson et al. (2014) proposes a decentralized hierarchical predictive control system that can handle models with several states, while keeping the computational complexity down. The vehicle speed and possible additional energy states are optimized in the top layer with a direct optimal control algorithm whereas gear shifts and engine on/off decisions are optimized in a lower control layer with a DP algorithm. To avoid the computational complexity of a mixed-integer problem, the direct optimal control algorithm in the top layer uses a powertrain model which is only physically accurate as long as the vehicle is driving with a preselected cruise gear; all lower gears are abstracted by using a lower efficiency for acceleration requests that exceed what can be delivered in the cruise gear. This modelling approach encourages the direct optimal control algorithm to avoid unnecessary gear shifts.

⋆ This research was supported by the Chalmers Energy Initiative and the Swedish Energy Agency.

This paper expands the control algorithm from (Johannesson et al., 2014; Murgovski et al., 2015) with predictive information of the movement pattern of surrounding vehicles. In order to add constraints that prevent the vehicle from colliding with slow traffic in front, it is required to model the relation between travelled time and travelled position at all samples along the prediction horizon. An exact model of this relation results in nonlinear equality constraints. To reach problem convexity the nonlinear constraints must be relaxed to inequality constraints.

Relaxing equality constraints to inequality constraints is a valid technique if it can be ensured that the solution of the resulting problem also satisfies the equality constraint. In the paper we investigate cases when the relaxation is and is not valid. For the cases when the relaxation is not valid, an affine approximation is proposed to model the relation between travelled time and travelled position, and the error of the approximation is investigated.

To reduce the complexity of the presentation, the paper only treats conventional vehicles. For information on how to expand the model to hybrid vehicles, see Johannesson et al. (2014).

2. OUTLINE AND CONTRIBUTION

The paper starts by introducing the notation in Section 3. The considered vehicle is described in Section 4 and modelled in Section 5. The control objective is introduced in Section 6 and the predictions of surrounding vehicles are modeled in Section 7. The hierarchical control architecture is briefly described in Section 8 and the optimization problem that is solved in the top layer is described in Section 9 with an alternative formulation in Section 10. Problem convexity is analyzed in Section 11 where also approximations required to reach a Linear Program (LP) are described. Simulations that support the analysis in Section 11 are presented in Section 12. The paper is concluded in Section 13.

Contribution: Besides the focus on conventional vehicles instead of hybrid vehicles, the contribution when compared to Johannesson et al. (2014); Murgovski et al. (2015) is how to include predictions of surrounding traffic while maintaining problem convexity.

3. NOTATION

The nomenclature used in the paper is as follows: the symbols F, P, and E describe force, power and energy, while the subscripts V, E, B, T, and A describe vehicle, internal combustion engine, the driveline retarder and mechanical brakes, transmission, and auxiliaries. The subscript d is added to denote dissipative terms, while the expression $(\cdot)$ denotes a function of variables. The vehicle velocity, v, and the signals describing force, power and energy are functions of time, although explicit notation is omitted for improved readability.

4. VEHICLE INFORMATION

The studied vehicle is a long haulage diesel truck with the main vehicle parameters given in Table 1. The truck is equipped with a 12 gear Automated Manual Transmission (AMT). The final drive ratio is decided so that gear 12 gives a favorable engine rpm when driving at about 80 km/h. When driving on the highway the truck will most of the time be in gear 12 which is therefore also referred to as the cruise gear.

Table 1. Vehicle parameters

Parameter	Value
Vehicle mass	$m = 40\,\text{tonne}$
Effective mass in cruise gear	$m_e = 40.03\,\text{tonne}$
Wheel radius	$R_w = 0.5\,\text{m}$
Aerodynamic drag coefficient	$c_d A_f = 5.2$
Rolling resistance coefficient	$c_r = 0.005$
Air density	$\rho_a = 1.184\,\text{kg/m}^3$
Gravitational acceleration	$g = 9.81\,\text{m/s}^2$
Engine maximum power	$P_{E\max} = 350\,\text{kW}$

5. VEHICLE MODEL

The vehicle is modelled as a point mass system with the longitudinal vehicle dynamics described by

$$m_e \dot{v} = F_V - F_{Vd}(\cdot) - mg\sin\alpha, \tag{1}$$

where F_V is the propulsion force, v is the longitudinal speed, α is the road gradient, g is the gravitational acceleration, m is the vehicle mass and m_e is the equivalent mass that includes the actual vehicle mass and terms reflecting inertia of rotational components. The vehicle is subject to dissipative (retarding) forces

$$F_{Vd}(\cdot) = \frac{\rho_a A_f c_d}{2} v^2 + mgc_r\cos\alpha \tag{2}$$

consisting of the aerodynamic drag and the rolling resistance; see Table 1 for parameter values.

The kinetic energy is given by

$$E_V = \frac{m_e v^2}{2}, \tag{3}$$

and the relation

$$\frac{dv}{dt} = v\frac{dv}{ds} = \frac{1}{2}\frac{d}{ds}v^2, \tag{4}$$

gives

$$\frac{dE_V}{ds} = F_V - mg\sin\alpha(s) - \frac{\rho_a A_f c_d E_V}{m_e} - mgc_r\cos\alpha(s). \tag{5}$$

Equation (5) can be discretized in distance based on the assumption that α and F_V are constant during the sample distance s_s (zero order hold). This yields

$$E_V(k+1) = E_V(k) + \\ \big(F_V - mg\sin\alpha(k) - \frac{\rho_a A_f c_d E_V}{m_e} - mgc_r\cos\alpha(s)\big)s_s. \tag{6}$$

Similarly, the time to travel one sample of length s_s with the kinetic energy E_V is given by

$$t_s = \frac{s_s}{\sqrt{2E_V/m_e}}. \tag{7}$$

resulting in the travel time

$$t(k+1) = t(k) + \frac{s_s}{\sqrt{2E_V(k)/m_e}}. \tag{8}$$

The force F_V is given by

$$F_V = F_E - F_B, \tag{9}$$

where F_E is the force from the engine, F_B is the force from the driveline retarder and mechanical brakes.

The forces are limited according to

$$F_{E,\min}\big(E_V,\kappa,P_{\mathrm{A}}\big) \le F_E \le F_{E,\max}\big(E_V,\kappa,P_{\mathrm{A}}\big), \quad \text{(10a)}$$

$$0 \le F_B \le F_{B,\max}(E_V), \quad \text{(10b)}$$

where $\kappa \in \{1,\dots,12\}$ is the gear number, $F_{E,\min}$ and $F_{E,\max}$ are the engine friction and maximum torque characteristics translated to act on the vehicle point mass, $F_{B,\max}$ is the maximum total brake force from the retarder and mechanical brakes, P_{A} is the mechanical alternator power that is drawn from the engine to supply the auxiliary systems.

The fuel consumption during one sample is modeled using a quasi-stationary assumption

$$E_{Ef} = f\big(F_E, E_V, \kappa\big). \quad (11)$$

6. CONTROL OBJECTIVE

For simplicity, it is assumed in this paper that the truck is driving on the highway on a segment with a constant speed limit. The driver inputs a desired average speed, v_{ref}, and corresponding maximum and minimum speeds $v_{\max}$, $v_{\min}$ to the cruise controller. In the paper, v_{ref} will be called the set speed.

The objective to be minimized by the predictive control system is a combination of the fuel consumption, a penalty on gear shifts, and a comfort penalty

$$\begin{aligned} J = \sum_{k=1}^{N} \Big(& E_{Ef}(k)\, s_s + h\big(\kappa(k), \kappa(k-1)\big) \\ & + w_C(\cdot, k)\Big), \end{aligned} \quad (12)$$

where N is the length of the prediction horizon and

$$\begin{aligned} w_C(k) = & \gamma_1 \Big(F_E(k) - F_B(k) \\ & - F_E(k-1) + F_B(k-1)\Big)^2 \end{aligned} \quad (13)$$

is the comfort penalty, E_{Ef} is the fuel consumption, and h is the gear shift penalty function. The penalty parameter $\gamma_1 \ge 0$, allow the controller to be tuned for increased comfort. Increasing γ_1 means that some of the fuel gains might be sacrificed for a smoother velocity trajectory without fast changes of the acceleration and driveline torque.

To prevent gear shifts that only result in small fuel gains at the expense of comfort and increased wear, the gear shift penalty function, h, can be set higher than the actual fuel energy required to execute a shift.

7. SURROUNDING TRAFFIC

Based on the assumption that the truck will stay in the lane and not overtake, predictions of the movement of vehicles in front can be translated to a lower bound on the travel time

$$t_{\min}(k) \le t(k), \quad (14)$$

where $t_{\min}(k), k \in \{1,\dots,N\}$ is the minimum travel time at each position along the prediction horizon which guarantees a safe distance or time lag to a vehicle in front. Similarly, an upper bound on the travel time

$$t_{\max}(k) \ge t(k), \quad (15)$$

can be introduced to guarantee a maximum time lag from the desired average speed entered by the driver, $v_{\mathrm{ref}}(k), k \in \{1,\dots,N\}$, or to guarantee a minimum time lag to the predicted motion of a proceeding vehicle.

8. CONTROL ARCHITECTURE

Problem (12) is a mixed-integer problem. It is desired to avoid the computational burden that is required to solve such problems. Therefore, a hierarchical control architecture is introduced that results in less computational complexity at the expense of a suboptimal solution to (12). The hierarchical control architecture has one real-time control layer that actuates the control decisions and two two predictive control layers that plan the speed and gear shift strategy and that operate on different time scales with different update frequencies, prediction horizons, and model abstractions.

The top control layer is responsible for planning a vehicle speed reference that is sent to the cruise controller as well as to the gear shift optimization which takes place in the lowe predictive control layer. At each update the optimization problem is initialized with the current dynamic state, the travel time, the desired total trip time (or desired average speed), information about road topography and speed limits as well as a prediction of the motion of surrounding vehicles within the prediction horizon. It is assumed that the prediction of the motion of surrounding vehicles is based on radar information and or vehicle to vehicle communication. To be able to react to changes in the predicted movement pattern of surrounding vehicles the optimization should be updated at about 5 Hz.

The lower predictive control layer is responsible for selecting a gear that minimizes (12) for the given speed reference. Since the speed reference is given from the optimization in the top layer and is assumed to be followed exactly, what remains is a low complexity optimization problem with only integer state variables: gear and engine on/neutral. This problem can be solved in real-time with DP, on currently available electric control units, using an update rate faster than 0.2 s and a prediction horizon of 1 km.

In the real time control layer, a cruise controller tracks the speed reference with a constraint on the distance to the vehicle in front. The cruise controller generates an acceleration request that is allocated to the engine, driveline retarder and mechanical brakes based on the priority to use the mechanical brakes as little as possible.

9. SPEED REFERENCE OPTIMIZATION

The speed reference optimization will only have an indirect impact on the gear shift cost, $\sum_{k=1}^{N} h\big(\kappa(k), \kappa(k-1)\big)$ in that the generated speed reference should avoid provoking gear shifts by not requesting unnecessary high acceleration. For a truck driving on the highway it is sufficient to accurately model the maximum torque characteristics on the preferred cruise gear; torque requests exceeding what can be delivered on the cruise gear is modeled with an artificial lower efficiency. The approach is thus to minimize an approximated version of the objective (12) where $\tilde{E}_{Ef}(\cdot,k)$ is introduced as approximation of $E_{Ef}(\cdot,k)+h(k)$. The details of the approximation is described in Section 9.1 and the required approximations for problem convexity is described in Section 11.

The optimization problem is formulated with the optimization variables: $F_E(k)$, $F_B(k)$, $k\in\{1,\ldots,N-1\}$ and $E_V(k)$, $t(k)$ $k\in\{1,\ldots,N\}$.

The optimization problem is then given as

$$\min \tilde{J}=\sum_{k=1}^{N}\Big(\tilde{E}_{Ef}(\cdot,k)+w_C(\cdot,k)\Big), \quad (16a)$$

subject to (6)-(11) and (14),(15),

$$E_V(1)=\frac{m_e v_0^2}{2},\quad t(1)=0, \quad (16b)$$

$$F_E(1)=F_{E,0},\quad F_B(1)=F_{B,0}, \quad (16c)$$

$$\frac{m_e\hat{v}_{min}^2(k)}{2}\le E_V(k),\ \forall k\in\{1,\ldots,N\}, \quad (16d)$$

$$E_V(k)\le\frac{m_e v_{\max}^2(k)}{2},\ \forall k\in\{1,\ldots,N\}. \quad (16e)$$

The lower limit on the vehicle speed, $\hat{v}_{\min}(k)$ as well as the allowed time window defined by (14) and (15) are set so that there always exists a feasible solution. The feasible solution with the feasible speed $\hat{v}$ is generated by a forward simulation of the system (6), (10), generating F_V from a stationary feedback that tries to maintain $\hat{v}$ close to the desired averge speed, v_{ref}, unless at a position directly behind a vehicle that travels with a speed lower than v_{ref}. In this situation the controller instead tries to keep a fixed distance to the vehicle in front. The minimum speed is adjusted based on the feasible solution $\hat{v}_{\min}(k)=\min\{v_{\min},\hat{v}(k)\}$ for all $k\in\{1,\ldots,N\}$. The maximum allowed travel time in (15) is either calculated to keep a time lag to the predicted motion of a proceeding vehicle or calculated as $t_{\max}(k)=t_{\text{ref}}+\sum_{j=1}^{k}s_s/\hat{v}(j), k\in\{1,\ldots,N-1\}$ and $t_{\max}(N)=\sum_{j=1}^{N}s_s/\hat{v}(j)$, where t_{ref} is the maximum allowed time lag from the feasible $\hat{v}$.

9.1 Engine and transmission model

This section describes the engine torque/force limitations and the approximate engine energy consumption, $\tilde{E}_{Ef}(\cdot,k)$.

The maximum wheel force that can be delivered from the engine depends both on the vehicle speed and the selected gear as shown in Figure 1. To avoid a mixed-integer problem all other gears except the most relevant cruise gear are abstracted in the model. This is done by modeling the traction force from the engine, F_E, with two force contributions

$$F_E=F_{E,1}+F_{E,2}, \quad (17)$$

where $F_{E,1}$ is the force that can be delivered when the vehicle is operated in cruise gear and $F_{E,2}$ is the additional force that can be delivered by selecting any lower gear.

The maximum wheel force that can be delivered from the engine when in cruise gear is shown with a dotted grey line in Figure 2. In the optimization problem the dotted grey line is approximated by the piece-wise linear concave function $F_{E,1,\max}(E_V)$, disregarding the non-concave behavior at low vehicle speed. In the simulations in Section 12, $F_{E,1,\max}$, is composed of only two linear pieces.

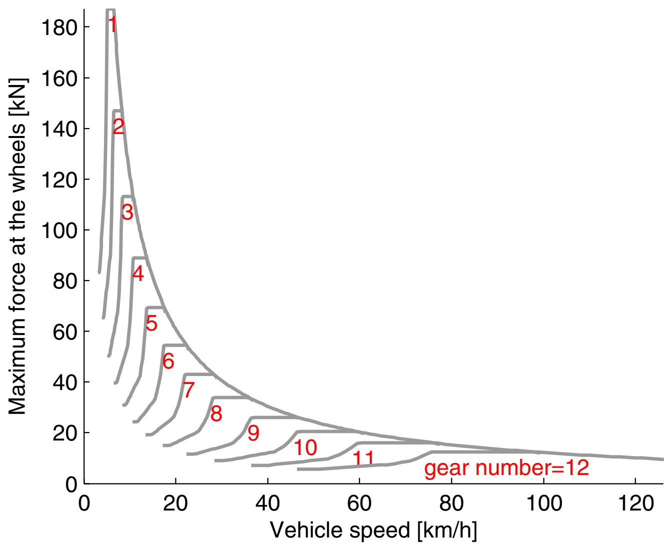

Fig. 1. The maximum wheel force from the engine as a function of the vehicle speed for all 12 gears. Due to the maximum power rating of the ICE the total maximum force at any gear is inversely proportional to the vehicle speed.

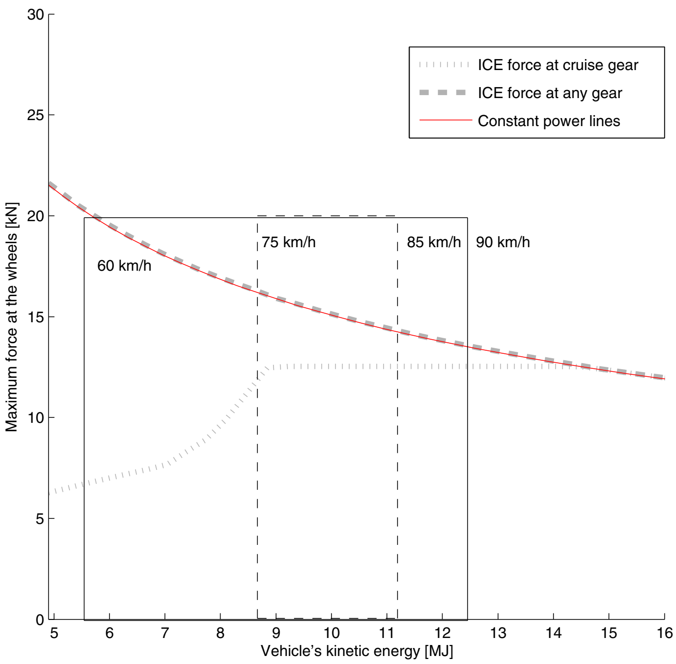

Fig. 2. The maximum wheel force from the engine as a function of the vehicle kinetic energy. The boxed areas corresponds to speed intervals from 60 km/h to 90 km/h and 75 km/h to 85 km/h. The curve 'ICE force at any gear' is the maximum engine force for any admissible gear at a specific speed.

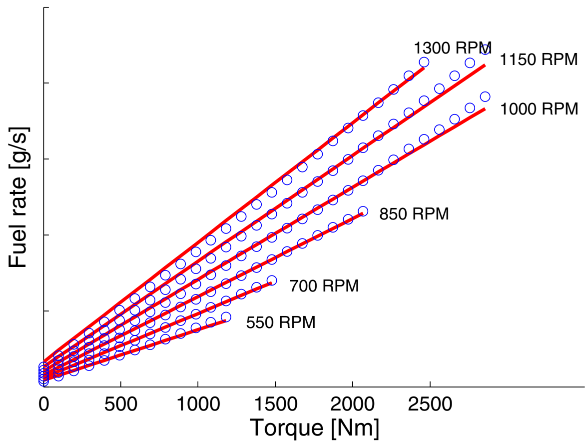

Fig. 3. Engine model versus measurements. The model is shown with red lines and the measured fuel mass rate with blue circles.

The engine friction when operated in cruise gear is modeled as affine in E_V,

$$T_{E,\text{fric}}(\cdot) = a_0 + a_1 E_V, \tag{18}$$

where $a_1 > 0$.

The engine torque/force constraints (10a) are then replaced with

$$F_{E,1} + \frac{P_A t_s}{s_s} \le F_{E,1,\max}(E_V) \tag{19a}$$

$$-\kappa_E T_{E,\text{fric}}(\cdot) = -\kappa_E\big(a_0 + a_1 E_V\big) \le F_{E,1} + \frac{P_A t_s}{s_s} \tag{19b}$$

$$F_{E,1} + F_{E,2} + \frac{P_A t_s}{s_s} \le \frac{P_{E\max}}{v} = \frac{P_{E\max}}{\sqrt{2E_V/m_e}} \tag{19c}$$

$$0 \le F_{E,2} \tag{19d}$$

where κ_E is a constant that transfers torque delivered at engine output to traction force acting on the vehicle point mass when the transmission is in cruise gear and where $P_{E\max}$ is the maximum rated engine power.

When in cruise gear, the engine energy consumption is modeled with a constant marginal efficiency

$$\tilde{E}_{Ef,1} = \frac{\left(F_{E,1} + \frac{P_A t_s}{s_s} + \kappa_E T_{E,fric}\right)s_s}{\eta_{E,1}} = \frac{\left(F_{E,1} + \frac{P_A t_s}{s_s} + \kappa_E(a_0 + a_1 E_V)\right)s_s}{\eta_{E,1}}. \tag{20}$$

Model (20) is fitted to measured data and compared with the measurements in Figure 3.

In order to encourage the optimization to, if possible, plan the driving with low enough acceleration so that the cruise gear can be kept, the additional force exceeding what can be delivered in the cruise gear is modeled with a lower marginal efficiency $\eta_{E,2} < \eta_{E,1}$. The result is the following engine energy consumption model:

$$\tilde{E}_{Ef}(\cdot) = \frac{\left(F_{E,1} + \frac{P_A t_s}{s_s} + \kappa_E(a_0 + a_1 E_V)\right)s_s}{\eta_{E,1}} + \frac{F_{E,2}s_s}{\eta_{E,2}}, \tag{21}$$

which is physically correct only when in cruise gear.

The engine energy consumption is the sum of the useful mechanical work $E_E = F_E s_s$ and the energy dissipation $\tilde{E}_{Ed}$:

$$\tilde{E}_{Ef} = E_E + \tilde{E}_{Ed} = (F_{E,1} + \frac{P_A t_s}{s_s} + F_{E,2})s_s + \tilde{E}_{Ed}. \tag{22}$$

Simple manipulations give the energy dissipation as

$$\tilde{E}_{Ed}(\cdot) = \Big(\big(F_{E,1} + \frac{P_A t_s}{s_s} + \kappa_E\,(a_0 + a_1 E_V)\big)/\eta_1 - F_{E,1} - \frac{P_A t_s}{s_s} + F_{E,2}\,(1/\eta_2 - 1)\Big)s_s, \tag{23}$$

which is linearly increasing in both E_V and t_s due to $1/\eta_1 > 1$ and $1/\eta_2 > 1$.

10. MINIMIZATION OF ENERGY DISSIPATION

An alternate view on problem (16) is given in this section. By making the dissipative terms

$$E_D(\cdot,k) = F_B s_s + F_{Vd}(\cdot,k)s_s + \tilde{E}_{Ed}(\cdot,k) \tag{24}$$

explicit in the objective function we show that problem (16) equivalently can be viewed as a minimization of the total energy dissipation. Using (6) and (9) the useful mechanical work from the engine can be expressed as

$$E_E(\cdot) = (F_V + F_B)s_s = E_V(k+1) - E_V(k) + F_B s_s + mg\sin\alpha(k)s_s + F_{Vd}(\cdot)s_s. \tag{25}$$

Objective (16) is then reformulated by replacing with expression (25):

$$\begin{aligned}\min \tilde{J} &= \sum_{k=1}^{N}\big(\tilde{E}_{Ef}(\cdot,k) + w_C(\cdot,k)\big)\\ &= \sum_{k=1}^{N}\big(E_E(\cdot) + \tilde{E}_{Ed}(\cdot,k) + w_C(\cdot,k)\big)\\ &= \sum_{k=1}^{N}\big(E_V(k+1) - E_V(k) + F_B s_s\\ &\quad + mg\sin\alpha(k)s_s + F_{Vd}(\cdot)s_s + \tilde{E}_{Ed}(\cdot,k) + w_C(\cdot,k)\big)\\ &= E_V(N+1) - E_V(1) + \sum_{k=1}^{N} mg\sin\alpha(k)s_s\\ &\quad + \sum_{k=1}^{N}\big(E_D(\cdot,k) + w_C(\cdot,k)\big),\end{aligned} \tag{26}$$

which shows that problem (16) is equivalent to minimizing the total energy dissipation.

11. CONVEX APPROXIMATIONS AND RELAXATIONS

Assuming that (10) is well described as affine in E_V, problem (16) is a non-convex problem due to the non-linear equality constraint (7) and the concave inequality constraint (19c). One approach is to solve problem (16) with Sequential Quadratic Programming (Nocedal and Wright, 2000). However, in order to get a better understanding of the problem it is worthwhile to investigate approximations and when convex relaxations of the nonconvex problem are valid.

First, to reach a convex problem formulation (19c) is linearized and replaced with

$$F_{E,1}(k) + F_{E,2}(k) + \frac{P_{\mathrm{A}} t_s}{s_s} \leq \Big(F_{E,\mathrm{tot},0}(k) + a_{F_E}(k) E_V(k)\Big), \tag{27}$$

where $F_{E,\mathrm{tot},0}(k)$ and $a_{F_E}(k)$ are position dependent coefficients with values given from the linearization.

By studying the curve 'ICE force at any gear' in Figure 2 it is evident that the linearization (27) is a reasonable approximation of (19c) over the narrow speed interval from 75 km/h to 85 km/h.

The second step is to investigate if equality will always hold when (7) is relaxed to

$$t_s(k) \geq \frac{s_s}{\sqrt{2E_V(k)/m_e}}, \tag{28}$$

which is a convex inequality constraint due to the convexity of $1/\sqrt{x}$.

Assume first that there is no vehicle in front. Then the relaxation is always valid, since the cost is linear in t_s. Assume now that there is a slowly moving vehicle in front of our vehicle so that (14) holds with equality for the optimal solution at sample N_1, or equivalently

$$\sum_{k=1}^{N_1} t_s(k) = t_{\min}(N_1), \tag{29}$$

which due to linearity means that all terms with $t_s(k)$ in the objective can be summed as

$$\sum_{k=1}^{N_1} P_A t_s(k)(1/\eta_{E,1} - 1) = P_A t_{\min}(N_1)(1/\eta_{E,1} - 1). \tag{30}$$

The cost directly associated with t_s up to sample N_1 will thus be defined by $t_{\min}(N_1)$ and is thereby unaffected by a possible inequality gap in (28) at one or more samples. Therefore, the argument that the cost is linear in t_s can no longer be used to prove that the relaxation is valid. Instead, the relaxation can only be shown valid in special cases when the F_B and $F_{E,2}$ is kept zero throughout the solution.

Since the relaxation is not always valid, an alternative is to approximate (7) with an affine equality constraint,

$$t_s(k) \approx b_0 + b_1 E_v(k). \tag{31}$$

Figure 4 shows the time error when approximating (7) with one affine function over the speed interval from 70 km/h to 90 km/h. The error is less than 2% which over a prediction horizon of 5 km when driving with an average speed of 80 km/h corresponds to a maximum position error at the end of the horizon of 100 m.

The only non-linear constraint in the problem formulation is constraint (7). This means that if (7) is approximated with an affine equality constraint the problem is turned into a linear program. In a real implementation, it is of interest to consider a penalty for jerk, which is natural to include with a quadratic penalty in the change in vehicle propulsion force. In that case the problem becomes a quadratic program (QP).

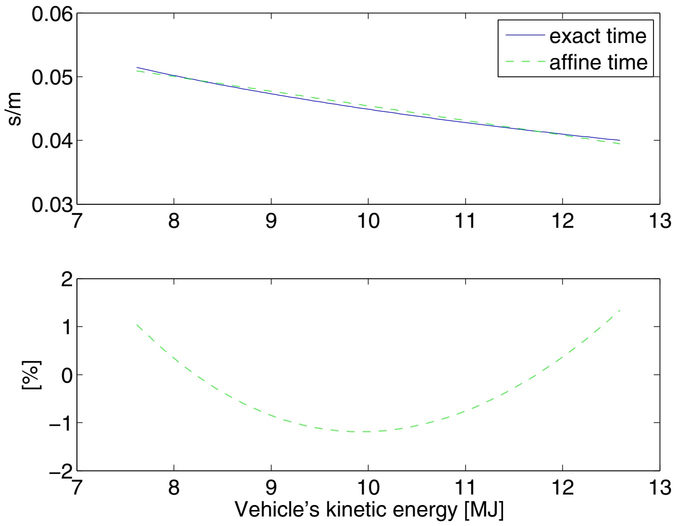

Fig. 4. Approximation of the sample time. The top window shows the sample time as a function of the kinetic energy and the bottom shows the error when approximating with an affine function.

12. SIMULATIONS

Due to lack of space the simulations only cover the speed reference optimization showing no simulations of the whole system with gear shift decisions and tracking of the reference speed. The simulations show the main characteristics of the optimal solutions and shows cases when the relaxation (28) is and is not valid. The simulations also show the solution with the affine approximation (31).

The studied scenario is as follows: The studied truck starts at the top of a hill with a slowly moving vehicle 13 seconds in front and there are two hills within the prediction horizon of 4 km. The reference speed is set to 80 km/h and the vehicle is allowed to over speed with 8 km/h. The vehicle in front is predicted to travel at 75 km/h and the minimum allowed time lag between the vehicles is set to 3 seconds.

Two variants of the speed reference optimization are studied. The first variant, shown in Figure 5 and 6 omits constraint (16d), with the result that there are no lower bounds on the kinetic energy. Instead, $t_{\max}(k), k \in \{1, \dots, N\}$ is set so that the maximum time lag from the feasible initial guess, labeled 'Initial guess' in Figure 5, is never allowed to exceed 5 seconds. The figures show that the optimal solution climbs the hills on cruise gear ($F_{E,2}(k) = 0, \forall k \in \{1, \dots, N\}$) and avoids activating the mechanical brakes ending up three seconds behind the vehicle in front at the end of the prediction horizon.

The second variant is presented in Figure 7 and 8 with the sole purpose to show that (28) does not necessarily hold with equality if F_B and $F_{E,2}$ are not zero at all times for the solution of the relaxed problem. In the optimization the speed in never allowed to go below 72 km/h unless when climbing the steep hill at the end of the prediction horizon. As seen in Figure 7 the optimization ends up being to 2.5 seconds behind the vehicle in front despite that the minimum allowed time lag between the vehicles is set to 3 seconds. The reason is that optimal solution satisfies (28)

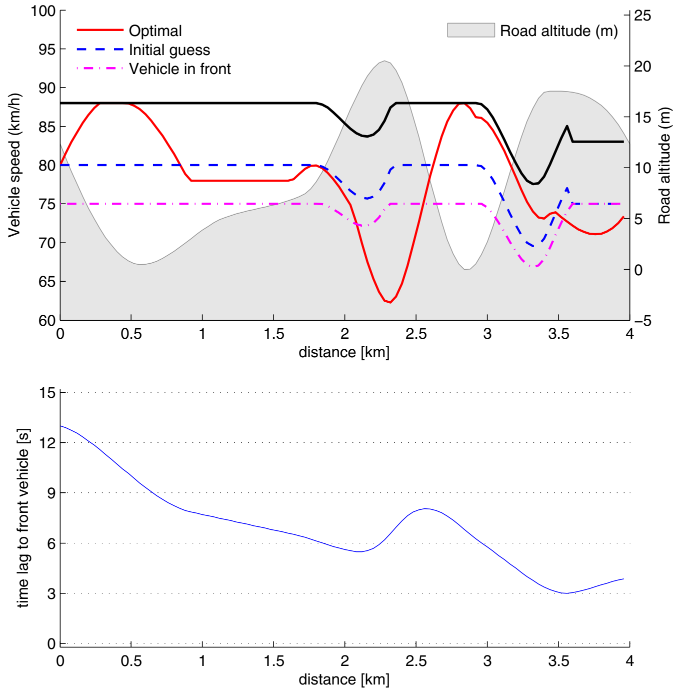

Fig. 5. Optimal speed reference with a maximum allowed time lag from the set speed of 5 seconds. The top window shows the speed trajectories on top of the road topography which is depicted in shaded grey. The lower window shows the time lag to the vehicle in front which is set to never be below 3 seconds.

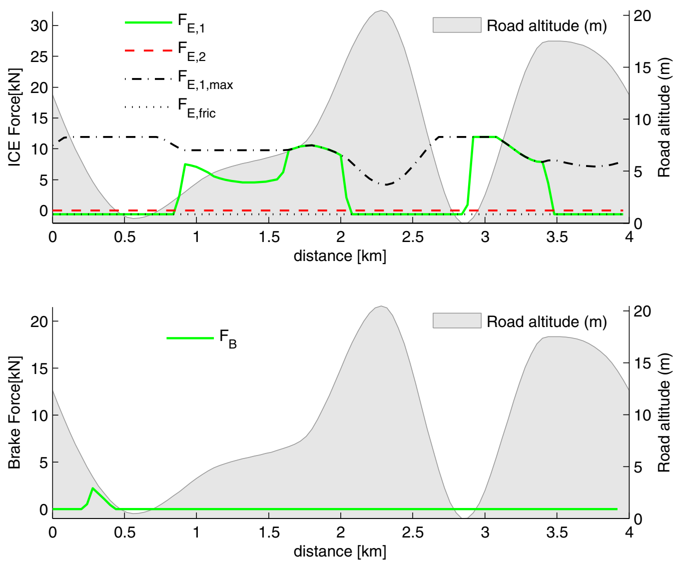

Fig. 6. Optimal force trajectories from an optimization with a maximum allowed time lag from the set speed of 5 seconds. The top window shows the engine force trajectories on top of the road topography which is depicted in shaded grey. The lower window shows the brake force trajectory.

with inequality resulting in an error in the relation between travelled time and travelled position.

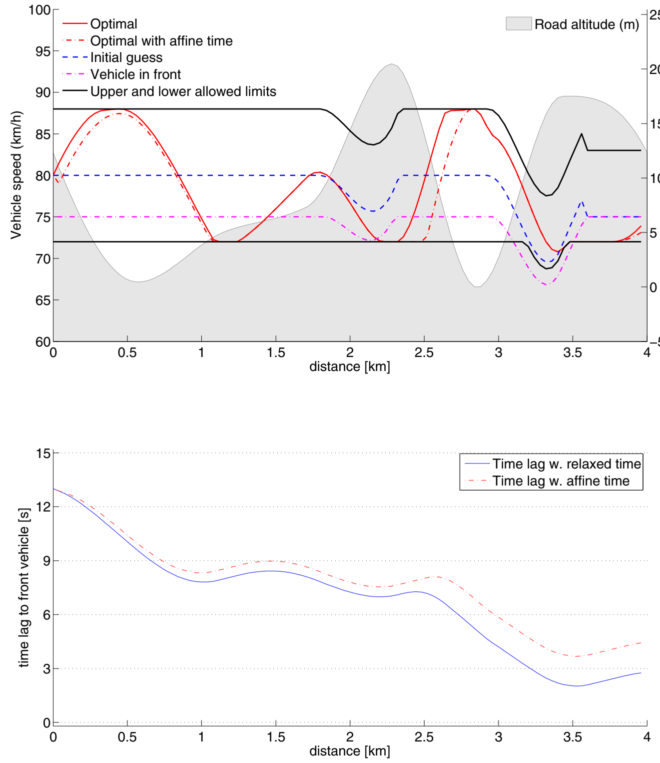

Fig. 7. Optimal speed reference with a minimum allowed speed of 72 km/h. The top window shows the speed trajectories on top of the road topography which is depicted in shaded grey. The lower window shows the time lag to the vehicle in front which is set to never be below 3 seconds. It is for this case verified that the time relaxation is not valid, while the affine approximation works better.

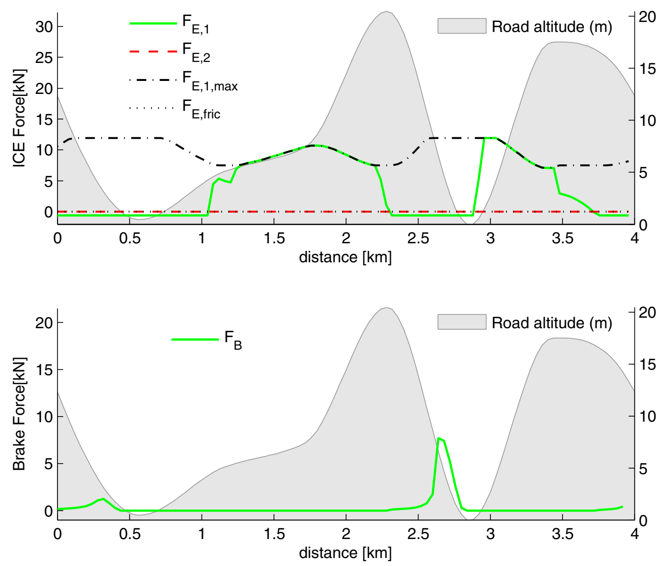

Fig. 8. Optimal force trajectories from an optimization with a minimum allowed speed of 72 km/h. The top window shows the engine force trajectories on top of the road topography which is depicted in shaded grey. The lower window shows the brake force trajectory.

13. CONCLUSION

The paper shows that predictions of the movement pattern of surrounding vehicles can be incorporated as a moving time window constraint when planning the vehicle speed reference in a convex optimization problem. By proposing an affine approximation of the relationship between time and kinetic energy, a time error of less than 2% can be held over the prediction horizon. This may be sufficient for planning purposes of platoons. If the problem is included in a model-predictive control formulation the error can be kept small by updating the solution frequently. In future work the speed reference optimization presented in the paper will be extended to vehicle platoons and the control of traffic flows.

REFERENCES

Barkenbus, J.N. (2010). Eco-driving: An overlooked climate change initiative. *Energy Policy*, 38, 762–769.

Bellman, R.E. and Dreyfus, S.E. (1962). *Applied Dynamic Programming*. Princeton University Press.

Bertsekas, D. (2000). *Dynamic Programming and Optimal Control*. Athena Scientific, Bellmont Massachusets.

Hellström, E., Åslund, J., and Nielsen, L. (2010). Design of an efficient algorithm for fuel-optimal look-ahead control. *Control Engineering Practice*, 18(11), 1318–1327.

Hellström, E., Ivarsson, M., Åslund, J., and Nielsen, L. (2009). Look-ahead control for heavy trucks to minimize trip time and fuel consumption. *Control Engineering Practice*, 17(2), 245–254.

Johannesson, L., Murgovski, N., Jonasson, E., Hellgren, J., and Egardt, B. (2014). Predictive energy management of hybrid long-haul trucks. *Submitted to Control Engineering Practice.*

Koot, M., Kessels, J., Jager, B.D., Heemels, W., Vanden-Bosch, P., and Steinbuch, M. (2005). Energy Management Strategies for Vehicular Electric Power Systems. *IEEE Transactions on Vehicular Technology*, 54(3), 771–782.

Murgovski, N., Johannesson, L., Egardt, B., and Sjöberg, J. (2015). Convex relaxations in the optimal control of electrified vehicles. In *In Proc. of the 2015 American Control Conference*. Chicago, IL, USA.

Nocedal, J. and Wright, S.J. (2000). *Numerical Optimization (Springer Series in Operations Research and Financial Engineering)*. Springer, Berlin.

Pettersson, N. and Johansson, K.H. (2006). Modelling and control of auxiliary loads in heavy vehicles. *International Journal of Control*.

Van Keulen, T., de Jager, B., and Steinbuch, M. (2011). Optimal trajectories for vehicles with energy recovery options. In *the 18th IFAC World Congress*. Milan, Italy.

Van Keulen, T., Foster, D., de Jager, B., and Steinbuch, M. (2010). Velocity Trajectory Optimization in Hybrid Electric Trucks. In *In Proc. of the 2010 American Control Conference*. Baltimore, USA.